2009

# Dynamic modelling of hydroelectric turbine-generator unit connected to a HVDC system for small signal stability analysis

Yin Chin Choo
*University of Wollongong*, ycc260@uow.edu.au

Ashish P. Agalgaonkar
*University of Wollongong*, ashish@uow.edu.au

Kashem Muttaqi
*University of Wollongong*, kashem@uow.edu.au

Sarath Perera
*University of Wollongong*, sarath@uow.edu.au

Michael Negnevitsky
*University of Tasmania*

## Publication Details

Y. Choo, A. P. Agalgaonkar, K. Muttaqi, S. Perera & M. Negnevitsky, "Dynamic modelling of hydroelectric turbine-generator unit connected to a HVDC system for small signal stability analysis," in AUPEC09: Proceedings of the 19th Australasian Universities Power Engineering Conference, 2009, pp. 1-6.

# Dynamic modelling of hydroelectric turbine-generator unit connected to a HVDC system for small signal stability analysis

**Abstract**

This paper presents the linearised small-signal dynamic modelling of hydroelectric turbine-generator (TG) unit with CIGRE first high-voltage direct current (HVDC) benchmark system in the synchronously rotating D-Q reference frame for small-signal stability analysis. The interaction behaviour between the hydroelectric unit and the dynamics and control of HVDC system is investigated utilising eigen-analysis,participation factor analysis and by conducting sensitivity studies. The computation of eigenvalues and eigenvectors for small signal stability analysis provides an invaluable insight onto the power system dynamic behaviour by characterising the damping and frequency of the system oscillatory modes. Theconsequences of different operating conditions, such as active and reactive power variations, the variation of generator-toturbine inertia ratio, as well as the changes of HVDC constant current controller parameters on small-signal system stability are investigated.

**Keywords**

Dynamic, modelling, hydroelectric, turbine, generator, unit, connected, HVDC, system, for, small, signal, stability, analysis

**Disciplines**

Physical Sciences and Mathematics

**Publication Details**

Y. Choo, A. P. Agalgaonkar, K. Muttaqi, S. Perera & M. Negnevitsky, "Dynamic modelling of hydroelectric turbine-generator unit connected to a HVDC system for small signal stability analysis," in AUPEC09: Proceedings of the 19th Australasian Universities Power Engineering Conference, 2009, pp. 1-6.

# Dynamic Modelling of Hydroelectric Turbine-Generator Unit connected to a HVDC System for Small Signal Stability Analysis

Y. C. Choo, A. P. Agalgaonkar, K. M. Muttaqi and S. Perera
Integral Energy Power Quality and Reliability Centre,
School of Electrical, Computer and Telecommunications Engineering,
University of Wollongong, NSW 2522, AUSTRALIA.
Email: ycc260@uow.edu.au

M. Negnevitsky
Centre for Renewable Energy and Power Systems,
School of Engineering,
University of Tasmania, Hobart 7005, AUSTRALIA.

***Abstract*—This paper presents the linearised small-signal dynamic modelling of hydroelectric turbine-generator (TG) unit with CIGRE first high-voltage direct current (HVDC) benchmark system in the synchronously rotating $D$-$Q$ reference frame for small-signal stability analysis. The interaction behaviour between the hydroelectric unit and the dynamics and control of HVDC system is investigated utilising eigen-analysis, participation factor analysis and by conducting sensitivity studies. The computation of eigenvalues and eigenvectors for small signal stability analysis provides an invaluable insight onto the power system dynamic behaviour by characterising the damping and frequency of the system oscillatory modes. The consequences of different operating conditions, such as active and reactive power variations, the variation of generator-to-turbine inertia ratio, as well as the changes of HVDC constant current controller parameters on small-signal system stability are investigated.**

## I. Introduction

Since the 1920s, power system stability has been a vital aspect of secure system operation [1]. System stability is defined as the ability of a power system, for a given initial operating condition, to regain a state of operating equilibrium after being subjected to a disturbance [1], [2]. A system is said to be small signal stable if the power system is able to remain in synchronism under small disturbances. A disturbance is considered to be small if the linearisation of the equations that depict the corresponding response of the system is permitted for the purpose of analysis [2], [3].

The small signal stability issue generally occurs due to inadequate damping of power system oscillations [2]. The dynamic characteristics of the power system can be determined from small-signal analysis using linearisation approaches, and damping controllers can be designed based on the information provided on system oscillatory modes.

The formulation of the linearised small-signal state space model of the integrated AC-DC systems can be established by linearising each power system components individually, transforming input-output variables into common reference frames, and establishing interaction relationship between different power system components [4]. The developed linearised dynamic model is used to analyse the interaction behaviour between the hydroelectric unit and HVDC link by manipulating the operating conditions, generator-to-turbine inertia ratio and controller parameters; the consequences of such variations are depicted in the eigenvalue trajectories. Eigenvalue analysis is used to identify the stability modes and damping characteristics of the integrated system. The dominant modes will be used to identify system stability limit for different operating conditions, generator-to-turbine inertia ratio and HVDC constant current controller parameters.

For power system analysis, the electrical network is normally represented by means of algebraic-equations in which inductances and capacitances are represented by their admittance at fundamental frequency. The dynamic representation of the electrical network based on linearised differential equations incorporated with linearised dynamic models of hydroelectric unit and HVDC system is applicable for the investigation of the high-frequency modes. The subsynchronous torsional interaction (SSTI) between turbine-generator torsional modes and the fast acting constant current controller of HVDC system may occur at high-frequency. The integrated linearised small-signal dynamic system developed in this paper has included the dynamic representation of shaft model, which allows the investigation of SSTI phenomena.

The small signal stability analysis of HVDC and static var compensators with their controllers has been addressed in [5]. Three different modelling approaches for CIGRE first HVDC benchmark model, namely linear-continuous-detailed model, linear-continuous-simplified model and linear discrete system model have been presented in [6]. The development of a linear continuous time state model of the small-signal dynamics of a HVDC system using modularisation techniques is detailed in [4]. A parallel ac-dc power system has been represented with reference to a rotor rotating reference frame in [7] and the capabilities and limitation of the analog computer in providing solutions to electromechanical problems have been outlined in [8]. Linearised modelling of turbine-generator shaft dynamics and HVDC system has been presented in [9] and [10] for subsynchronous oscillation analysis.

The main purpose of this paper is to present the modelling techniques, which depict the dynamic characteristics of hydroelectric turbine-generator (TG) unit and HVDC systems using linearised state space models. This allows the investigation of the small-signal stability aspects associated with the control interaction between the hydroelectric unit and the HVDC system at higher frequencies, using eigen-analysis. The paper is structured as follows. Section II illustrates the analytical methodologies for small signal stability analysis. Section III describes the mathematical modelling of the hydroelectric unit and HVDC system, which includes detailed representation of governor, turbine, exciter, power system stabiliser (PSS), torsional shaft model, AC filter, electrical system, converter system and current controller. Section IV elaborates the integrated study system involving hydroelectric power system and CIGRE first HVDC benchmark model and simulation results are presented by applying small disturbances to the study system. The paper is concluded in section V.

## II. Small-Signal Stability Analysis

This section elaborates the small signal stability analysis of a power system when subjected to small disturbances. Analytical methodologies used to determine the small signal stability are eigenanalysis, participation factors analysis and sensitivity analysis. Eigen properties such as damping ratio and oscillation frequency associated with system modes are revealed as well.

### A. Eigenanalysis

The eigenvalues of the system are the values of $\lambda$ that fulfil the characteristic equation of system matrix $A_{sys}$:

$$det(\lambda I - A_{sys}) = 0 \tag{1}$$

The analysis of the eigen properties in matrix $A_{sys}$ reveals vital information on the system stability characteristics. A pair of eigenvalues is represented as $\lambda = \sigma \pm j\omega$, where its oscillation frequency and damping ratio are established as $f = \frac{\omega}{2\pi}$ and $\zeta = \frac{-\sigma}{\sqrt{\sigma^2+\omega^2}}$ respectively. System stability can be guaranteed if all the system eigenvalues lie onto left-half plane, i.e. Re$(\lambda_i) < 0$ for all $i$ [2], [3].

### B. Participation Factor Analysis

Participation matrix, which combines both left and right eigenvectors, is a non-dimensional scalar that measures the correlation between the state variables and the modes of a linear system. It implies the relative involvements of the respective states in the corresponding modes. This is described as [2], [3]:

$$P = [p_1,\ p_2\ \ldots\ p_n] \tag{2}$$

with $p_i = [p_{1i},\ p_{2i}\ \ldots p_{ni}]^T = [\phi_{1i}\psi_{i1},\ \phi_{2i}\psi_{i2}\ \ldots \phi_{ni}\psi_{in}]^T$ where, $\phi_{ki}$ = $k^{th}$ entry of the right eigenvector $\phi_i$; and $\psi_{ik}$ = $k^{th}$ entry of the left eigenvector $\psi_i$.

$\phi_{ki}$ evaluates the activity of the $k^{th}$ state variable in the $i^{th}$ mode, while $\psi_{ik}$ weighs the contribution of this activity to the mode [2].

## III. Linearised State Space Models of Hydroelectric Turbine-Generator and HVDC Link

The formulation of the linearised state space model for the integrated system involves linearisation of each subsystem, transformation of input-output variables into common reference frames, and interconnection of the subsystems [4]. Similar techniques have been employed in this paper for formulation of the system state equations. Integration of the subsystems can be carried out as the input-output of a subsystem can be the output-input of another subsystem. Note that the Park's components $f_{dq}$ and the Kron's components $f_{DQ}$ will be used conventionally throughout the paper, where $f$ can be any variable. Subscripts $dq$ and $DQ$ are used to denote variables in rotor and synchronous reference frames, respectively.

### A. Modelling of Hydroelectric Turbine-Generator

A three-phase salient pole synchronous machine, with its equivalent circuits of $dq$-axes as shown in Fig. 1, is modelled to represent the hydroelectric TG unit. The established linearised machine model has the following state-space representation:

$$\begin{aligned} \Delta\dot{x}_{hydro} &= [A_{hydro}]\,\Delta x_{hydro} + [B_{hydro1}]\,\Delta E_{fd} \\ &\quad + [B_{hydro2}]\,\Delta u_{hydro} \end{aligned} \tag{3}$$

$$\Delta y_{hydro} = [C_{hydro}]\,\Delta x_{hydro} \tag{4}$$

where, $\Delta x_{hydro} = [\Delta\psi_d\ \Delta\psi_q\ \Delta\psi_{fd}\ \Delta\psi_{kd}\ \Delta\psi_{kq}]^T$, $\Delta u_{hydro} = [\Delta v_d\ \Delta v_q]^T$, $\Delta y_{hydro} = [\Delta i_d\ \Delta i_q]^T$, $A_{hydro}$, $B_{hydro}$ and $C_{hydro}$ are the state, control or input and output matrices respectively for a hydro unit. $E_{fd}$ is the field voltage, $\psi_d$ and $\psi_q$ are the stator flux linkages per second, $\psi_{fd}$, $\psi_{kd}$ and $\psi_{kq}$ are rotor flux linkages per second for a field winding and damper windings repectively, $v_{dq}$ and $i_{dq}$ are voltages and currents in $dq$ reference frame respectively.

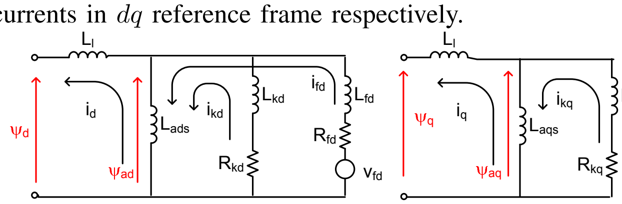


Fig. 1. Equivalent circuits of dq-axes for hydroelectric unit

### B. Modelling of Mechanical System

The linearised model of the hydroelectric torsional shaft system is represented based on a mass-spring-damping model as follows:

$$\Delta\dot{x}_{shaft} = [A_{shaft}]\Delta x_{shaft} + [B_{shaft}]\Delta u_{shaft} \tag{5}$$

$$\Delta y_{shaft} = [C_{shaft}]\Delta x_{shaft} \tag{6}$$

where, $\Delta x_{shaft} = [\Delta\omega_{gen}\ \Delta\omega_{tur}\ \Delta\delta_{gen}\ \Delta\delta_{tur}]^T$, $\Delta y_{shaft} = [\Delta\omega_{gen}\ \Delta\delta_{gen}]^T$, $\Delta u_{shaft} = [\Delta P_m\ \Delta P_e]^T$, $A_{shaft}$, $B_{shaft}$, $C_{shaft}$ are the state, control or input and output matrices respectively for the mechanical system. $\omega$ and $\delta$ are the rotor speed and angle. $P_m$ and $P_e$ are the mechanical and electrical powers respectively. Subscripts '$gen$' and '$tur$' represent generator and turbine respectively.

*C. Modelling of Electrical System*

The linearised representation of the excitation system (exciter and PSS) and governor-turbine can be expressed as:

$$\begin{aligned}\Delta\dot{x}_e &= [A_e]\Delta x_e + [B_e]\Delta u_e &(7)\\ \Delta y_e &= [C_e]\Delta x_e + [D_e]\Delta u_e &(8)\end{aligned}$$

where, $x_e$, $y_e$, $u_e$ are the state, output and input vectors of the excitation and governor-turbine system, $A_e$, $B_e$, $C_e$ and $D_e$ are the state, control or input, output and feedforward matrices respectively for the excitation and governor-turbine system.

The AC side filters can be represented in terms of a shunt capacitor with reactance $X_{Cfilter}$. The state space representation of the rectifier side AC system (in terms of $DQ$ components of different variables) can be expressed as follows:

$$\begin{aligned}\Delta\dot{x}_N &= [A_N]\Delta x_N + [B_N]\Delta u_N &(9)\\ \Delta y_N &= [C_N]\Delta x_N &(10)\end{aligned}$$

where, $\Delta x_N = [\Delta v_D \ \Delta v_Q]^T$, $\Delta y_N = [\Delta v_D \ \Delta v_Q]^T$, $\Delta u_N = [\Delta i_D \ \Delta i_Q \ \Delta i_{hvdcD} \ \Delta i_{hvdcQ}]^T$, $A_N, B_N, C_N$ are the state, control or input and output matrices respectively for the electrical system. $v_D$, $v_Q$ are the bus voltages represented in $DQ$ reference frame at the rectifier ac side, $i_{DQ}$ and $i_{hvdcDQ}$ are generator and HVDC currents in $DQ$ reference frame respectively.

The currents $i_{CDQ}$ flowing through the ac filter at rectifier side are decided by the power system components connected to the bus. Hydroelectric unit is connected directly to the bus, and a HVDC link as well in this study system. Thus, generator and HVDC currents are the inputs to the system.

$$\Delta i_{CDQ} = \Delta i_{DQ} - \Delta i_{hvdcDQ} \quad (11)$$

*D. Modelling of HVDC System*

The HVDC system can be represented in terms of a T-model as shown in Fig. 2. The linearisation of the dynamic equations for the HVDC system including the constant current (CC) controller of rectifier, yields equations (12), (13) and (14). The CC controller has a phase-locked loop (PLL) associated to it, which provides a more stable operation [10]. The phase lag resulting from PLL is represented by $\alpha_{PLL}$. The dynamics of CC and PLL are depicted in Fig. 3.

$$\begin{aligned}\Delta\dot{x}_{hvdc} &= [A_{hvdc}]\Delta x_{hvdc} + [B_{hvdc1}]\Delta u_{hvdc1}\\ &\quad + [B_{hvdc2}]\Delta u_{hvdc2} + [B_{hvdc3}]\Delta u_{hvdc3} &(12)\\ \Delta y_{hvdc1} &= [C_{hvdc1}]\Delta x_{hvdc} + [D_{hvdc11}]\Delta u_{hvdc1}\\ &\quad + [D_{hvdc12}]\Delta u_{hvdc2} &(13)\\ \Delta y_{hvdc2} &= [C_{hvdc2}]\Delta x_{hvdc} + [D_{hvdc21}]\Delta u_{hvdc1}\\ &\quad + [D_{hvdc23}]\Delta u_{hvdc3} &(14)\end{aligned}$$

where, $\Delta x_{hvdc} = [\Delta I_{dcr} \ \Delta I_{dci} \ \Delta V_{dcm} \ \Delta\alpha_{CCI} \ \Delta\theta_{PLL}]^T$, $\Delta u_{hvdc1} = [\Delta I_{ord} \ \Delta\gamma]^T$, $\Delta u_{hvdc2} = [\Delta V_{acr} \ \Delta\theta_{Vacr}]^T$, $\Delta u_{hvdc3} = [\Delta V_{aci} \ \Delta\theta_{Vaci}]^T$, $\Delta y_{hvdc1} = [\Delta I_{acr} \ \Delta\theta_{Iacr}]^T$, $\Delta y_{hvdc2} = [\Delta I_{aci} \ \Delta\theta_{Iaci}]^T$, $A_{hvdc}$, $B_{hvdc}$, $C_{hvdc}$ and $D_{hvdc}$ are the state, control or input, output and feedforward matrices respectively for the HVDC system. $I_{dc}$ is the direct current, $V_{dcm}$ is the DC voltage on the dc line, $\alpha_{CCI}$ is the rectifier angle output from the integral controller, $\theta_{PLL}$ is the PLL output angle, $I_{ord}$ is the reference current, $\gamma$ is the inverter extinction advance angle, $V_{ac}$ and $\theta_{Vac}$ are the AC line-to-line voltages and the phasor associated at the converter bus, $I_{ac}$ and $\theta_{Iac}$ are the AC line current flowing through the converter transformer and its associated phasor, subscripts $r$ and $i$ represent rectifier and inverter respectively.

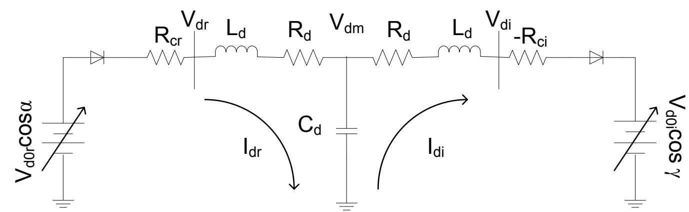


Fig. 2. HVDC System

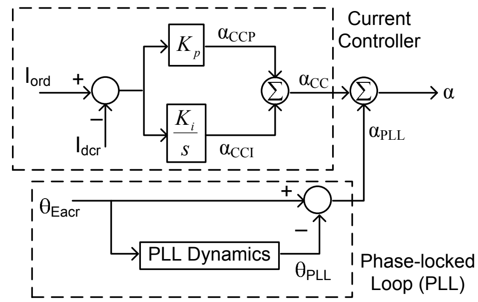


Fig. 3. Converter Control

*E. Interface Between AC and DC Systems*

The linearised state space model for each subsystem has been represented individually as shown in subsections III-A, III-B, III-C and III-D. The linearised representation of the ac-dc interaction equations, as in equations (15) and (16), highlights the small-signal inter-relationship between ac and dc systems as shown below:

$$\begin{aligned}\Delta I_{acr} &= \frac{\sqrt{6}}{\pi} B_r T_r \Delta I_{dcr} &(15)\\ \Delta\phi_{acr} &= -\frac{X_{cr} I_{dcr0}}{\sqrt{2} T_r V_{acr0}^2 sin(\phi_{acr0})}\Delta V_{acr} + &(16)\\ &\quad \frac{sin(\alpha_0)}{sin(\phi_{acr0})}\Delta\alpha + \frac{X_{cr}}{\sqrt{2} T_r V_{acr0} sin(\phi_{acr0})}\Delta I_{dcr}\end{aligned}$$

Since each subsystem is represented in a different reference frame, it is important to transform all the variables into common reference frame before the integration of different subsystems. The linearised transformation between variables in $DQ$ reference frame and polar coordinates is shown in equation (17).

$$\begin{bmatrix}\Delta f_D\\ \Delta f_Q\end{bmatrix} = \begin{bmatrix} sin\theta_{fac0} & f_{ac0}cos\theta_{fac0}\\ cos\theta_{fac0} & -f_{ac0}sin\theta_{fac0}\end{bmatrix}\begin{bmatrix}\Delta f_{ac}\\ \Delta\theta_{fac}\end{bmatrix} \quad (17)$$

The linearised transformation from synchronously rotating reference frame to rotor reference frame is expressed in equation (18) [11]. The relationship among variables in rotor, synchronous reference frames and polar coordinates is illustrated in Fig. 4.

$$\begin{bmatrix}\Delta f_d\\ \Delta f_q\end{bmatrix} = \begin{bmatrix} cos\delta_0 & sin\delta_0\\ -sin\delta_0 & cos\delta_0\end{bmatrix}\begin{bmatrix}\Delta f_D\\ \Delta f_Q\end{bmatrix} + \begin{bmatrix}\Delta f_{q0}\\ -\Delta f_{d0}\end{bmatrix}\Delta\delta \quad (18)$$

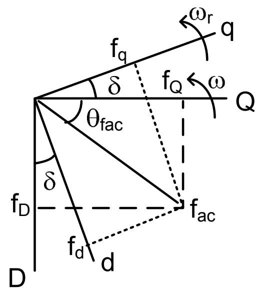


Fig. 4. Phasor diagram of the relationship among variables in $dq$, $DQ$ reference frames and polar coordinates

## IV. Simulation Results

A hydroelectric TG unit connected to a HVDC system as shown in Fig. 5 is used as the study system for small signal stability analysis. This study system comprises of a 500 kV, 1000 MW monopolar DC link and a 1210 MVA hydroelectric system. The HVDC system is represented by the CIGRE first HVDC benchmark model. It is assumed that the rectifier operates at constant current (CC) control mode whilst the inverter operates at constant extinction angle (CEA) control mode.

The hydroelectric unit on the rectifier ac side composes of turbine-generator, governor, excitation system, power system stabiliser (PSS) and shaft system. The overall system comprises of 30 state variables.

Analytical methodologies, such as eigenanalysis, participation factor and sensitivity analyses, are utilised to investigate the interaction behaviour between the hydroelectric unit and the dynamics and control of HVDC system. The consequences of different operating conditions, such as active and reactive power variations, as well as the variations of generator-to-turbine inertia ratio $n$ and the changes of HVDC constant current controller parameters $K_p$ and $K_i$ on small-signal stability are investigated in this paper.

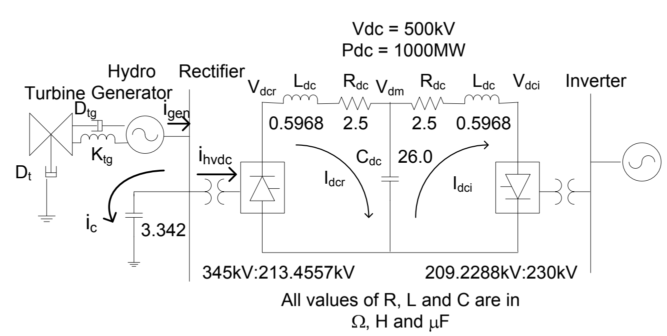


Fig. 5. A Hydro Turbine-Generator Unit Interconnected to CIGRE First HVDC Benchmark Model

### A. Eigenvalue and Participation Factor Analyses for Initial Operating Condition

This subsection reveals the eigenvalues of each subsystem individually and for an interconnected system at an initial operating condition. The eigenvalue analysis distinctively allows the investigation of how each power system component influences the overall system eigenvalues. Tables I and II shows the eigenvalues of hydroelectric unit and HVDC system independently. The eigenvalue modes 5 and 6 of hydroelectric unit are the local plant mode of oscillation, which has an oscillation frequency of 2.0475 Hz and a damping ratio of 0.0699. The modes 1, 2 and 3, 4 in Table II represent the dynamics of the HVDC link while mode 5 represents the time constant of the PLL.

Some of the selective eigenvalues for the integrated system are shown in Table III. Modes 12 and 13 are the torsional modes of the hydroelectric unit, and they are critically damped but are generally stable. This corresponds to a hydroelectric system with generator-to-turbine inertia ratio $n$ of 10. Such torsional modes have an oscillation frequency of 6.22 Hz.

TABLE I
Eigenvalues of Hydroelectric Unit

| Mode | Real($\lambda$) | Imag($\lambda$) | $f$ (Hz) | Damping ratio, $\sigma$ |
|---|---|---|---|---|
| 1,2 | -12.49 | ± j313.49 | 49.8935 | 0.0398 |
| 3 | -50.09 | j0.00 | 0.00 | 1.0000 |
| 4 | -47.10 | j0.00 | 0.00 | 1.0000 |
| 5,6 | -0.90 | ± j12.86 | 2.0475 | 0.0699 |
| 7 | -0.55 | j0.00 | 0.00 | 1.0000 |

TABLE II
Eigenvalues of HVDC System

| Mode | Real($\lambda$) | Imag($\lambda$) | $f$ (Hz) | Damping ratio, $\sigma$ |
|---|---|---|---|---|
| 1,2 | -38.23 | ± j346.91 | 55.2129 | 0.1095 |
| 3,4 | -35.08 | ± j69.47 | 11.0568 | 0.4507 |
| 5 | -25.00 | j0.00 | 0.00 | 1.0000 |

TABLE III
Selective eigenvalues of the interconnected system

| Mode | Real($\lambda$) | Imag($\lambda$) | $f$ (Hz) | Damping ratio, $\sigma$ |
|---|---|---|---|---|
| 1 | -1.000 | j0.0 | 0.00 | 1.000 |
| 2,3 | -13.854 | ± j2292.5 | 364.86 | 0.006 |
| 4,5 | -16.980 | ± j1607.0 | 255.76 | 0.011 |
| 6,7 | -38.275 | ± j346.8 | 55.20 | 0.110 |
| 8 | -111.396 | j0.0 | 0.00 | 1.000 |
| 9,10 | -35.146 | ± j69.5 | 11.06 | 0.451 |
| 11 | -52.430 | j0.0 | 0.00 | 1.000 |
| 12,13 | -0.000 | ± j39.1 | 6.22 | 0.000 |
| 14 | -36.698 | j0.0 | 0.00 | 1.000 |
| 15 | -34.392 | j0.0 | 0.00 | 1.000 |
| 16,17 | -13.133 | ± j14.7 | 2.35 | 0.665 |
| 18 | -28.515 | j0.0 | 0.00 | 1.000 |
| 19 | -29.412 | j0.0 | 0.00 | 1.000 |
| 20 | -25.000 | j0.0 | 0.00 | 1.000 |

Figs. 6, 7 and 8 shows the participation factor analysis on hydroelectric unit, HVDC system and the overall system respectively. This analysis reveals the relative involvements of the respective states in the corresponding modes. The participation factor analysis on the overall system as seen in Fig. 8 shows that state variables 24 and 25 contributes the most onto mode 20 associated with the exciter. The next highest contribution is from state variable 24 onto mode 3 associated with the hydro unit. State variables 24 and 25 are voltage variables of PSS. This suggests that PSS has a considerable effects onto modes 3 and 20.

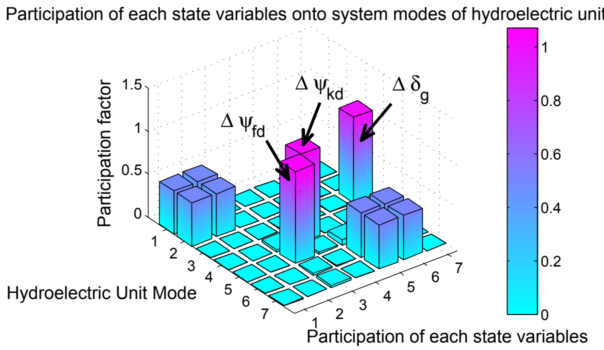


Fig. 6. Participation factor analysis on hydroelectric unit

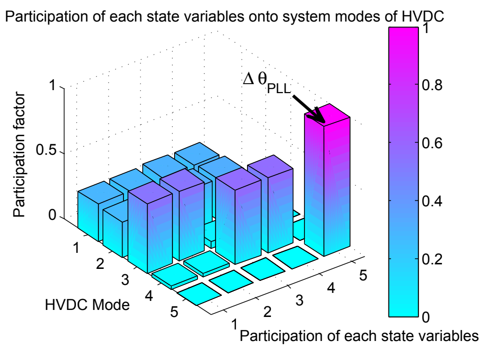


Fig. 7. Participation factor analysis on HVDC system

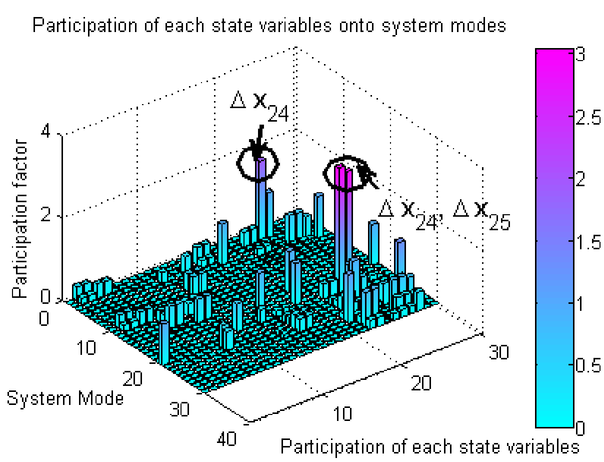


Fig. 8. Participation factor analysis on overall system

### B. Sensitivity Analysis for Different Operating Conditions

Different operating conditions have considerable effects on system small-signal stability. In reality, small disturbances always occur in a power system, such as small variations of load and generation. Thus, it is important to investigate the influence of system operating conditions on the overall small-signal stability. In this study, the system is subjected to active ($P$) and reactive power ($Q$) changes and system least stable modes will be used as an indicator for stability. Two cases have been considered: isolated hydroelectric system and interconnected hydroelectric system with HVDC system.

Simulation results for influence of $PQ$ variations on system small-signal stability for isolated and interconnected operations are shown in Figs. 9 and Fig. 10 respectively. In an isolated operation, the local plant mode (swing mode) oscillations are used as the stability indicator. The torsional modes are used as the stability indicator for interconnected operation as they appears to be the critical modes in the system. It is observed in Fig. 9 that the swing mode is not affected substantially by the $PQ$ variations. It is well-damped for both leading and lagging power factor conditions. However, the swing mode frequency increases slightly for an increment of active power. On the contrary, the critical modes of the overall system are sensitive to the $PQ$ changes as seen in Fig. 10. For low $P$ injection into the system, it is more susceptible to instability due to insufficient damping and the negative damping introduced by HVDC converter controls. Increase in $Q$ may result in instability.

The torsional modes of the system appear to be system critical mode. Damping controller can be designed based on the information provided on system oscillatory modes, and incorporated to provide more damping into the system.

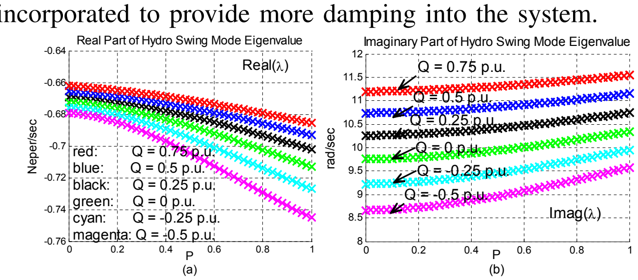


Fig. 9. Swing mode for hydroelectric unit subject to PQ variation

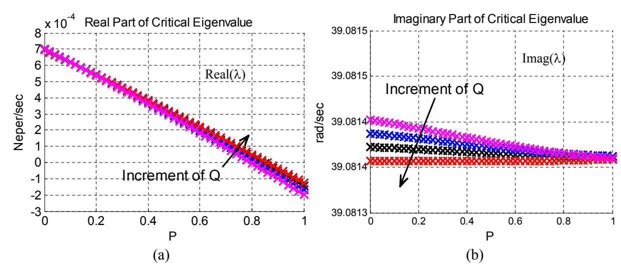


Fig. 10. Critical mode of overall system subject to PQ variation

### C. Effects of Different Generator-to-Turbine Inertia Ratio

It has been demonstrated in the earlier studies [12] that the hydro units with a low generator-to-turbine inertia ratio $n$ would experience SSTI problem, which is due to the lack of damping at the torsional frequency $f_n$. This subsection illustrates the consequences of $n$ variation on the small-signal stability. In this study, generator inertia $H_{gen}$ is 3.0 sec and remains the same for all $n$ values. It is the turbine inertia $H_{tur}$ that varies throughout the studies. Fig. 11 shows that with an increasing value of $n$, torsional modes tend to shift more to the stable region. However, at $n$ = 30, the damping begins to reduce (indicated by the reduction of torsional modes real part). The increment of $n$ does improve the damping of the torsional modes. The simulation results also indicate that the hydro unit connected in the close vicinity of the HVDC system can possibly experience SSTI problem as the torsional modes for the integrated system have relatively low damping due to the negative damping introduced by CC controller. This can be evidently seen in Table IV.

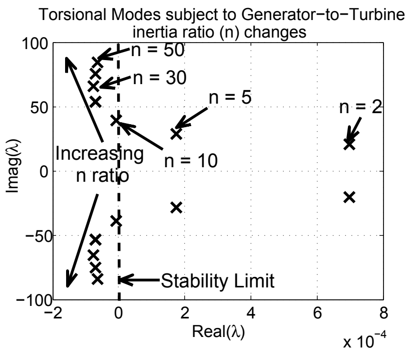


Fig. 11. Torsional modes of the hydroelectric unit subject to variation of generator-to-turbine inertia ratio ($n$)

TABLE IV
SYSTEM TORSIONAL MODES FOR DIFFERENT GENERATOR-TO-TURBINE INERTIA RATIO ($n$)

| $n$ | Real($\lambda$) | Imag($\lambda$) | $f$ (Hz) | Damping ratio, $\sigma$ |
|---|---|---|---|---|
| 2 | 6.9907e-4 | ± j20.404 | 3.247 | -3.4261e-5 |
| 5 | 1.7341e-4 | ± j28.862 | 4.594 | -6.0082e-6 |
| 10 | -6.2582e-6 | ± j39.080 | 6.220 | 1.6014e-7 |
| 20 | -7.0500e-5 | ± j54.000 | 8.594 | 1.3056e-6 |
| 30 | -7.5738e-5 | ± j65.609 | 10.442 | 1.1544e-6 |
| 40 | -7.0400e-5 | ± j75.450 | 12.008 | 9.3307e-7 |
| 50 | -6.2438e-5 | ± j84.153 | 13.393 | 7.4196e-7 |

### *D. Effects of Constant Current Controller Parameters*

The level and the frequency range of negative damping for the ac-dc system are dependent on the value of the firing angle [12]. Thus, the variation of HVDC constant current controller parameters, $K_p$ and $K_i$ on small-signal stability are also examined in the paper. Fig. 12 shows the trajectory of the critical system mode, which is identified as the torsional mode, subject to the variation of HVDC constant current controller parameters $K_p$ and $K_i$ at rectifier side. It is observed that the damping of the system critical mode can be improved utilising a low value of $K_p$ and $K_i$. The mode has less damping with an increment value of $K_p$. It is seen in Fig. 12(b) that with $K_p$ less than 8.5, all values of $K_i$ ranged from 10 - 100 will result in a stable system.

## V. CONCLUSIONS

This paper presents linearised small-signal dynamic models of hydroelectric system connected to a HVDC system. The eigenvalue analysis has been used as an analytical technique for small signal stability analysis of a sample hydroelectric system connected to CIGRE first HVDC benchmark model. The dynamic system response for different operating conditions, generator-to-turbine inertia ratio and HVDC constant current controller parameters has been investigated. The modal analysis for varying P and Q generation demonstrates that the swing mode of the isolated hydro operation does not get affected substantially. On the contrary, the critical modes of the integrated system, identified as torsional modes, are sensitive to the PQ variations and HVDC constant current controller parameters. It has also been demonstrated that the hydro units with low generator-to-turbine inertia ratio may experience SSTI problem due to dominant negative damping imposed by HVDC converter controls.

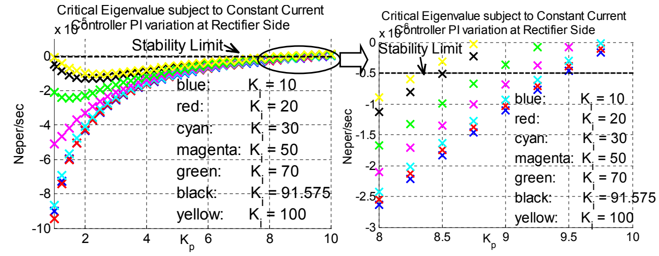


(a) (b)

Fig. 12. Critical mode of overall system subject to constant current PI controller variation

## ACKNOWLEDGMENT

This research has been funded by the Australian Research Council under ARC Discovery Grant K0014733, “Australian Research Council - Optimising Control of Hydroelectric Turbines Subject to Basslink Instability”.

## REFERENCES

[1] IEEE/CIGRE Joint Task Force on Stability Terms and Definitions, “Definition and Classification of Power System Stability,” *IEEE Transactions on Power Systems*, Vol. 19, No. 2, pp. 1387-1401, May 2004.

[2] P. Kundur. *Power System Stability and Control*. McGraw-Hill, 1994.

[3] Y.C. Choo, K.M. Muttaqi, M. Negnevitsky, “Evaluation of small signal stability of a power system,” *Australian Journal of Electrical and Electronics Engineering*, Vol. 4, No. 3, 2008.

[4] C. Osauskas, A. Wood, “Small-Signal Dynamic Modeling of HVDC Systems,” *IEEE Transactions on Power Delivery*, Vol. 18, No. 1, pp. 220-225, January 2003.

[5] S. Arabi, G.J. Rogers, D.Y. Wong, P. Kundur, M.G. Lauby, “Small Signal Stability Program Analysis of SVC and HVDC in AC Power Systems,” *IEEE Transactions on Power Systems*, Vol. 6, No. 3, pp. 1147-1153, August 1991.

[6] D. Jovcic, “Control of High Voltage DC and Flexible AC Transmission Systems,” *PhD Thesis*, The University of Auckland, December 1999.

[7] H.A. Peterson, P.C. Krause, “A Direct- and Quadrature-Axis Representation of a Parallel AC and DC Power System,” *IEEE Transactions on Power Apparatus and Systems*, Vol. PAS-85, No. 3, pp. 210-225, March 1966.

[8] H.A. Peterson, P.C. Krause, J.F. Luini, C.H. Thomas, “An Analog Computer Study of a Parallel AC and DC Power System,” *IEEE Transactions on Power Apparatus and Systems*, Vol. PAS-85, No. 3, pp. 191-209, March 1966.

[9] K.R. Padiyar. *Analysis of Subsynchronous Resonance in Power Systems*. Kluwer Academic Publishers, 1999.

[10] D.J. Kim, H.K. Nam and Y.H. Moon, “A Practical Approach to HVDC System Control for Damping Subsynchronous Oscillation Using the Novel Eigenvalue Analysis Program,” *IEEE Transactions on Power Systems*, Vol. 22, No. 4, pp. 1926-1934, November 2007.

[11] P.C. Krause. *Analysis of Electric Machinery*. McGraw-Hill, 1986.

[12] Y.C. Choo, A.P. Agalgaonkar, K.M. Muttaqi, S. Perera, M. Negnevitsky, “Subsynchronous Torsional Behaviour of a Hydraulic Turbine-Generator Unit Connected to a HVDC System,” *Proceedings of Australasian Universities Power Engineering Conference (AUPEC 2008)*, Sydney, New South Wales, 14-17 December, 2008.